Late-Twentieth-Century Climatology and Trends of Surface Humidity and Temperature in China

JULIAN X. L. WANG AND DIAN J. GAFFEN

NOAA Air Resources Laboratory, Silver Spring, Maryland

(Manuscript received 22 May 2000, in final form 15 October 2000)

ABSTRACT

Climatological surface temperature and humidity variables for China are presented based on 6-hourly data from 196 stations for the period of 1961–90. Seasonal and annual means for daytime, nighttime, and the full day are shown. The seasonal cycle of moisture is primarily controlled by the east Asia monsoon system, with dominant factors of temperature change in northern and western China and of moisture advection associated with monsoon circulations in the southeast.

Trends during 1951–94 are estimated for each station and for four regions of the country, with attention paid to the effects of changes in instrumentation, observing time, and station locations. The data show evidence of increases in both temperature and atmospheric moisture content. Temperature and specific humidity trends are larger at nighttime than daytime and larger in winter than summer. Moisture increases are observed over most of China. The increases are several percent per decade for specific humidity, and several tenths of a degree per decade for temperature and dewpoint. Increasing trends in summertime temperature and humidity contribute to upward trends in apparent temperature, a measure of human comfort.

1. Introduction

Studies of global and regional surface temperature and humidity variations provide insight into important aspects of the global climate system. Surface humidity and temperature regulate evaporation and transpiration processes and so have obvious connections to both the hydrological cycle and surface energy budget. Human comfort and health are influenced by temperature and humidity variations, particularly in summer.

Nevertheless, there is a lack of quality controlled climatological surface humidity data suitable for analysis of climatological variability and trends. For example, the comprehensive, global surface climatological datasets recently compiled by New et at. (1999, 2000) include only vapor pressure as a moisture variable, and, at many stations, rely on conversion from relative humidity and temperature, often not simultaneously measured. Existing analyses of surface climatology in China (e.g., Zhu 1962; Chen 1988) do not include humidity variables. Several recent studies of China's climate focused on surface temperature and precipitation (Zhai and Ren 1999; Zhai et al. 1999) and humidity in the free atmosphere (Zhai and Eskridge 1997). Among recent global tropospheric humidity climatologies (Ross and Elliott 1996; Randel et al. 1996), only Peixoto and Oort (1996) include surface data, but only relative humidity.

This paper is a companion to the study by Gaffen and Ross (1999), which presented a comprehensive surface temperature and humidity climatology over the United States for 1961–90 and assessed trends during 1961–95. Here we present climatologies of surface temperature and humidity variables for China for 1961–90 and trends during 1951–94.

2. Data

Surface weather observations, provided by the China Meteorological Administration to the U.S. Department of Energy's Carbon Dioxide Information Analysis Center, form the basis for this analysis. The station distribution is shown in Fig. 1, and a relevant description of the dataset is referred to Kaiser (1991). The 6-hourly observations at 0200, 0800, 1400, and 2000 Beijing Time (BT), are available covering the period 1951–94. Prior to 1961, two changes in observing protocols occurred: in 1960 all thermometers were lowered from 2 to 1.5 m, and from January 1954 to July 1960 the observation times were different (Portman 1993). The impact of these changes on trends is explored below.

We employ the 6-hourly surface pressure (p), surface temperature (T), and relative humidity (RH) data and compute dewpoint temperature (T_d), specific humidity (q), vapor pressure (e), and apparent temperature (T_a).

Corresponding author address: Julian X. L. Wang, NOAA Air Resources Laboratory, R/ARL, 1315 East–West Highway, Silver Spring, MD 20910.
E-mail: julian.wang@noaa.gov

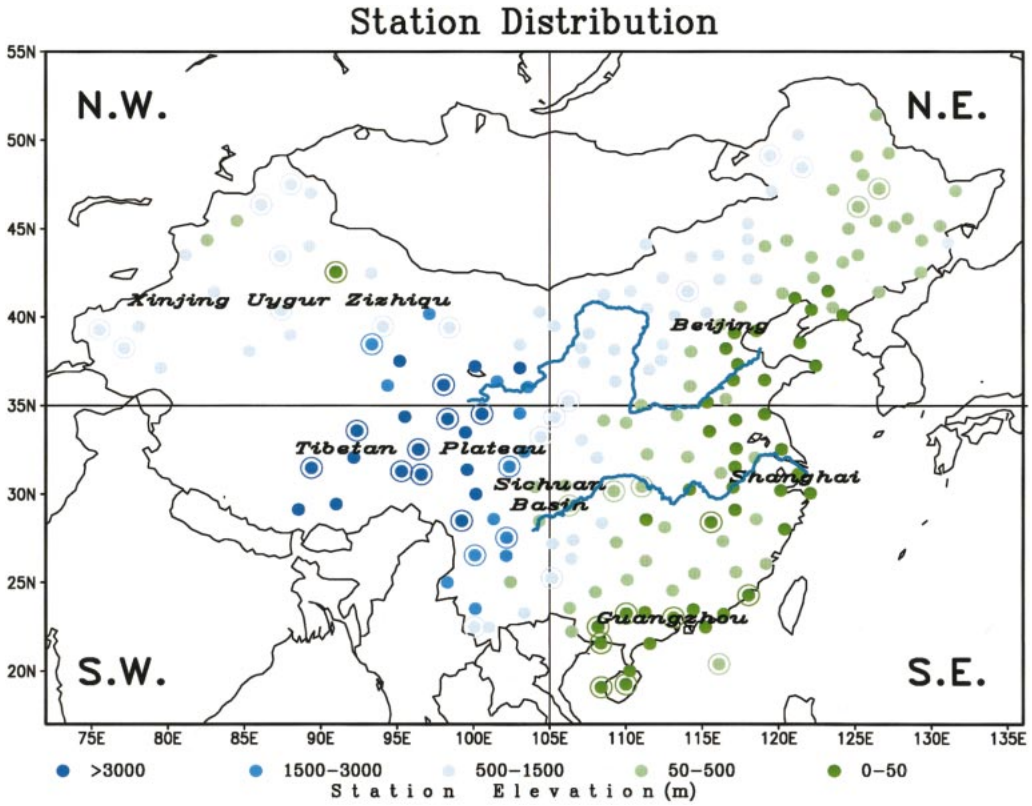

FIG. 1. Geographical distribution of 196 stations used in the study. Color shading indicates station elevation, and an outer circle indicates that certain records from a station were adjusted for abrupt changes associated with station relocation. Four regions described in the text are also shown.

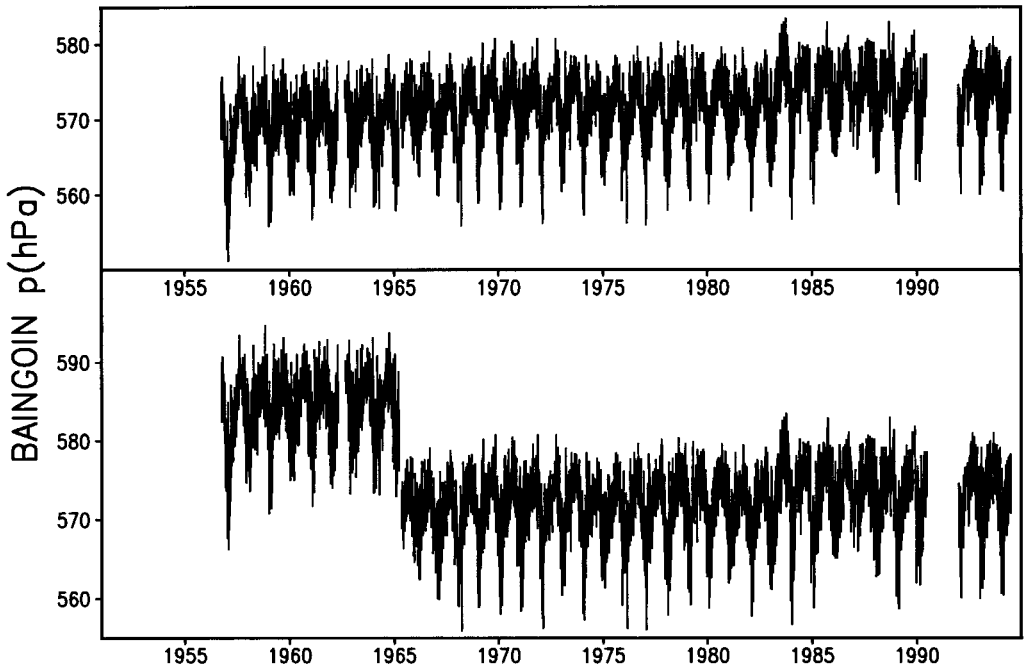

FIG. 2. Surface pressure measurements from Baingoin, China (31.48°N, 89.40°E), (top) after and (bottom) before adjustment. The data were adjusted by subtracting 12 hPa from the data for the period prior to 1 Apr 1965.

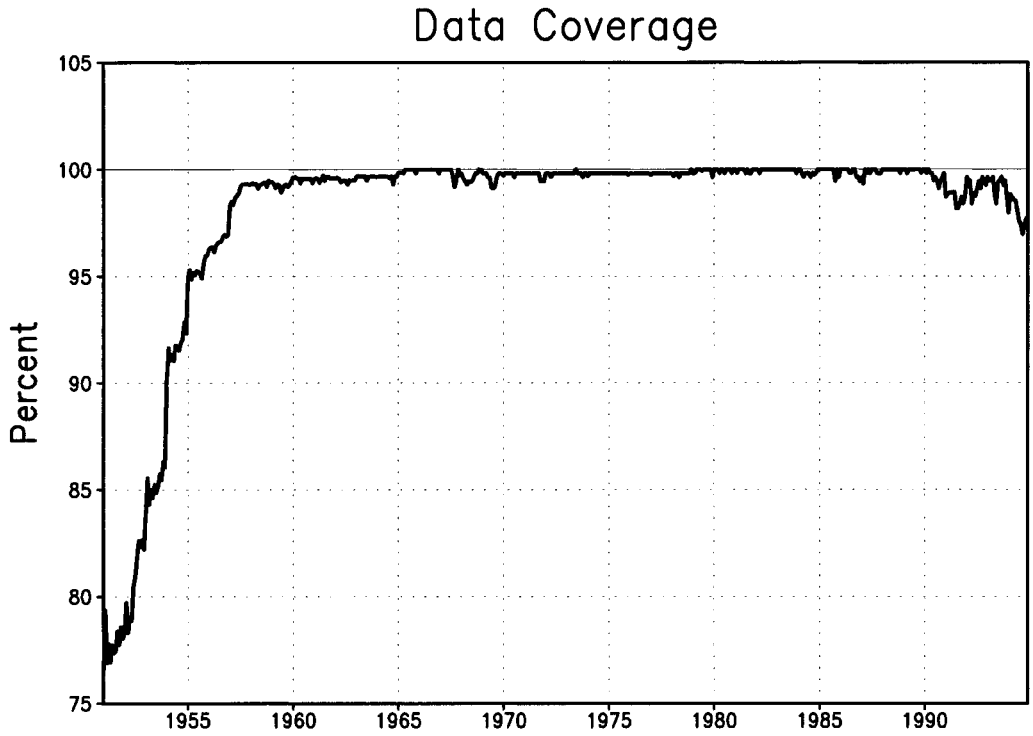

FIG. 3. Monthly percentage of 6-hourly data available for the 196-station network used in this study.

For T_a we ignore the effects of wind and radiation and use Steadman's (1984) regression equation $T_a = -1.3 + 0.92T + 2.2e$, where T is in degrees Celsius and e is in kiloPascals.

A relatively stable network of stations and consistency in operational procedure since 1961 ensure that the quality of surface observations in China, for climate studies, is generally good. However, we identified two types of erroneous data. The first is outlier data, inconsistent with the rest of the record, probably due to errors in data observing and transmitting procedure. Errors of this sort were identified by visual inspection of those data exceeding 3 standard deviations, and these data were rejected. The second type involved an abrupt shift in mean values, associated with changes in station location, which was evident in a limited station history information. An example is given in Fig. 2, showing 1400 BT surface pressure for Baingoin in Tibet. During April of 1965, the station was relocated from 31.48°N, 89.4°E to 31.23°N, 90.01°E, and the station elevation was also changed from 4380 to 4700 m. In these cases we adjusted the time series by shifting the earlier part of the time series by the difference in the mean values before and after the relocation. In almost all cases, the adjustments involved p and e data, and in one case T data were adjusted. In all cases, the effect of the adjustment was to reduce the magnitude of trends in the data. The network of 196 stations used for the analysis of climatology and trends is shown in Fig. 1, along with station elevation. The 28 stations (14% of the total) shown with a ring around the circle location indicator in Fig. 1 required data adjustments due to relocation.

From 1960 to 1990, each of the station records is at least 99% complete. During 1951–55, more data are missing (largely because only 0800, 1400, and 2000 BT observations were made during 1951–53, but even during these early years the record is more than 80% complete, as shown in Fig. 3. Below we present climatological values based on data for 1961–90 and trends for the entire period, 1951–94. Climatological monthly and seasonal [December–January–February (DJF), etc.] means are computed separately for the full day (daily mean based on all 6-hourly data), for daytime (based on 1400 BT data), and for nighttime (based on 0200 BT data). We also analyze trends and variations in four large regions, delineated by the 105°E meridian and by the 35°N parallel, and defined as northeast (NE), southeast (SE), southwest (SW), and northwest (NW), shown in Fig. 1.

3. Climatology

a. Specific humidity

Figure 4 shows the long-term annual mean (Fig. 4a), and the amplitude of the annual cycle (the range between maximum and minimum 30-yr-mean monthly values, Fig. 4b) of specific humidity q, the mass of water vapor per unit mass of moist air. The moistest region is in southern China, and values up to 10 g kg^{-1} extend as

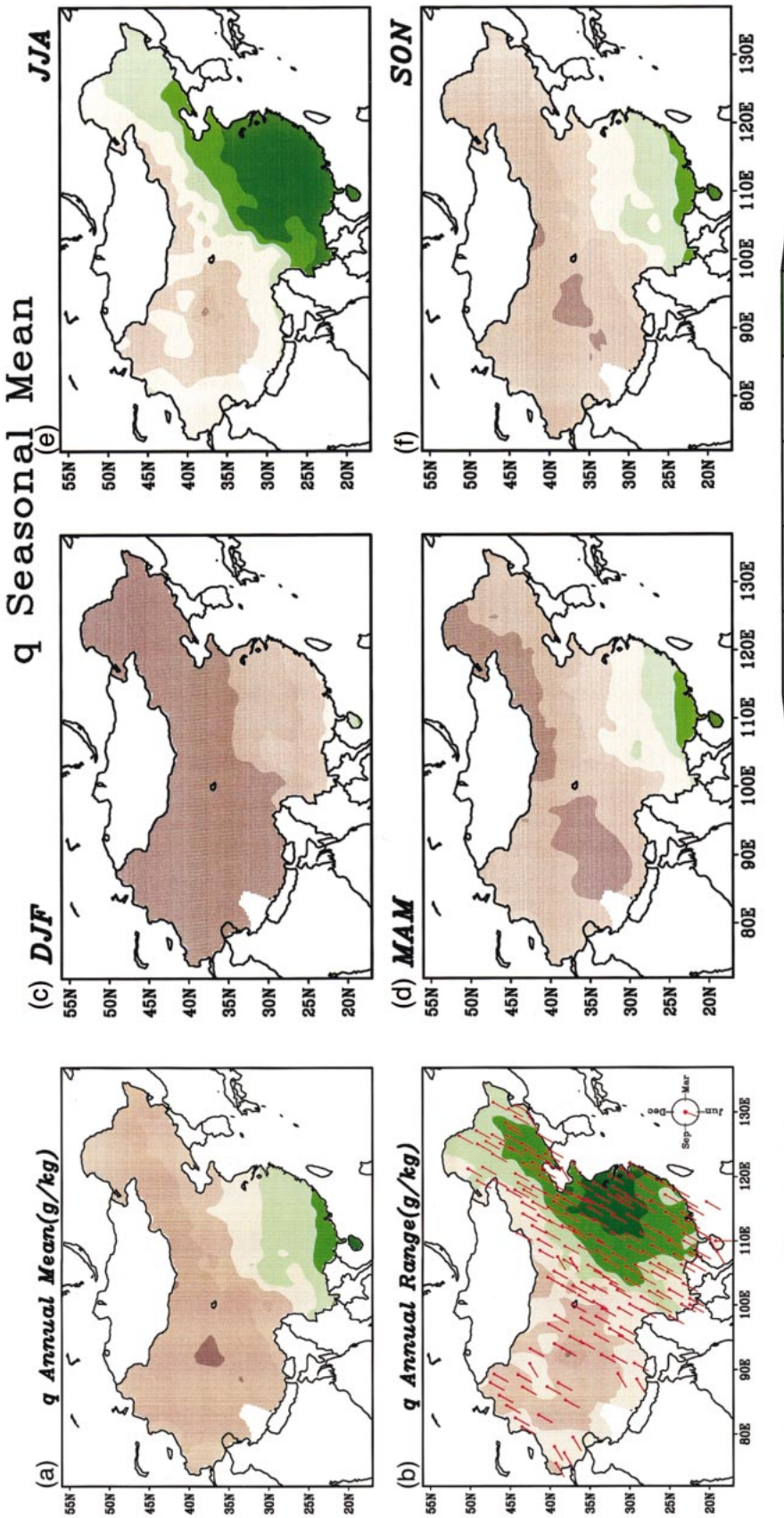

FIG. 4. (a) Climatological annual-mean specific humidity (g kg^{-1}). (b) Annual range of specific humidity, and the month of maximum, indicated by the clock direction of the line segment. Climatological specific humidity for (c) winter, (d) spring, (e) summer, and (f) autumn. All values are based on 1961–90 data for the full day.

TABLE 1. Climatological mean values of specific humidity, relative humidity, dewpoint, temperature, and apparent temperature in China, based on data for 1961–90. Values are shown for daytime, nighttime, and full day.

	q (g kg^{-1})	RH (%)	T_d (°C)	T (°C)	T_a (°C)
Day	7.0	48.7	2.3	14.4	14.6
Night	7.1	73.1	2.6	7.6	8.0
Full day	7.1	64.1	2.6	10.2	10.5

far north as the Yangtze River basin and west to the foot of the Tibetan Plateau. Much of northern and western China has annual-mean humidity values less than 6 g kg^{-1}. The annual range of q is largest (>10 g kg^{-1}) in eastern China (east of 105°E), particularly over the lower Yangtze and Yellow Rivers. July is the month of maximum q for most stations, although it is August for a few stations (Fig. 4b). Daytime and nighttime means and ranges of the specific humidity (figures not shown) are very similar to those in Fig. 4a, and day–night differences in annual-mean values are 0.1 g k^{-1}, which is less than 2% of the full-day values for China as a whole (Table 1). The magnitude of annual-mean q values and the spatial pattern of variability over China are remarkably similar to those features for the United States at comparable latitude (Gaffen and Ross 1999), except that the month of maximum q is generally August in the United States and July in China.

Four seasonal-mean q maps are presented in Figs. 4c–4f. Highest values are found in JJA, when q exceeds 10 g kg^{-1} over much of eastern China east of 100°E. This suggests a moisture supply mainly from the South China Sea and the East China Sea, consistent with the well-documented monsoon circulations of this region (Tao and Chen 1987). Values exceeding 17 g kg^{-1} are found over southeastern China and the Sichuan basin in JJA. There is a relatively high moisture region over southern Tibet, which may suggest the moisture sources from the Bay of Bengal (Murakami 1957; Asakura 1971). In winter (DJF), q values are less than 1 g kg^{-1} over most of northeast China and the Tibetan Plateau. Humidity changes between summer and winter are fairly symmetric, although the slightly higher values in SON than in MAM suggest a lag in q with respect to the seasonal march of solar elevation, as was found in the United States (Gaffen and Ross 1999).

b. Relative humidity

In contrast with q, RH has significant diurnal variability. On nationwide average, annual-mean RH is 48% for daytime, with a standard deviation (over all stations) of 13%, and 73% for nighttime, with a standard deviation of 14%. The day–night differences in RH are larger than the amplitude of the seasonal cycle, as shown in Fig. 5a, which also illustrates the presence of semiannual changes, especially in the daytime seasonal cycle curve. The relative contributions of annual and semiannual harmonics to the variance of seasonal cycle, shown in Table 2, indicates that the semiannual harmonic component accounts for as much as 26.5% of the total seasonal variance of daytime RH, based on the average of all stations. This is in marked contrast with each of the other variables, for which the semiannual harmonic explains only a few percent of the variance of the mean seasonal cycle.

Because of the evident existence of semiannual component, as well as abrupt shifts in RH in the spring and autumn at some stations, seasonal cycle of the relative humidity is a somewhat misleading notion, and values of annual range can not be defined exclusively. Therefore, instead of showing seasonal-mean maps, we present the annual means (Fig. 5b) and the mean seasonal cycles for each of the four regions (Figs. 5c,d,e,f). High values of annual-mean, daily mean RH (>60%) are seen in southeastern China from the coast extending westward to Tibet and northward to the Yellow River (Fig. 5b), where there is little seasonal variation, but much stronger diurnal variation, in RH (Fig. 5f); in northeastern China, the semiannual harmonic accounts for a relatively large fraction (>20%) of the total variance (Fig. 5d). The summertime maximum in this northeastern region is due to abundant moisture supply from the oceans to the south, and the secondary maximum in winter is associated with low temperature. For northwestern China (Fig. 5c), the temperature effect dominates and summertime moisture transport is responsible for a secondary maximum in July. Over southwestern China (Fig. 5e) summertime moisture transport from the Bay of Bengal is the major factor in seasonal RH changes.

c. Dewpoint temperature

Dewpoint temperature (T_d) means and seasonal changes depend on air temperature, moisture content, and atmospheric pressure. The spatial pattern of annual-mean T_d (Fig. 6a) is similar to that of q (Fig. 4a), with high T_d in southeastern China, and low T_d in Tibet. Like q, T_d reaches maximum values at most stations in July (Figs. 4b and 6b). However, because of the influence of T, the spatial distribution of the annual range of T_d (Fig. 6b) is quite different than for q (Fig. 4b). Generally, the largest annual changes in T_d occur at high latitudes.

Seasonal means (Figs. 6c–f) of T_d combine aspects of the seasonal patterns of q and T. For example, the strong seasonal T cycle in northern China (Fig. 7) dominates the seasonal T_d cycle. In southern China, the seasonal cycle of T_d resembles that of q (Figs. 4b–e). Like q, the average day–night difference in T_d is small, with an annual-mean, station-mean value of about 0.3 K.

d. Temperature and apparent temperature

Seasonal-mean T patterns for China are shown in Figs. 7a–d. During the winter (DJF), the isotherms are

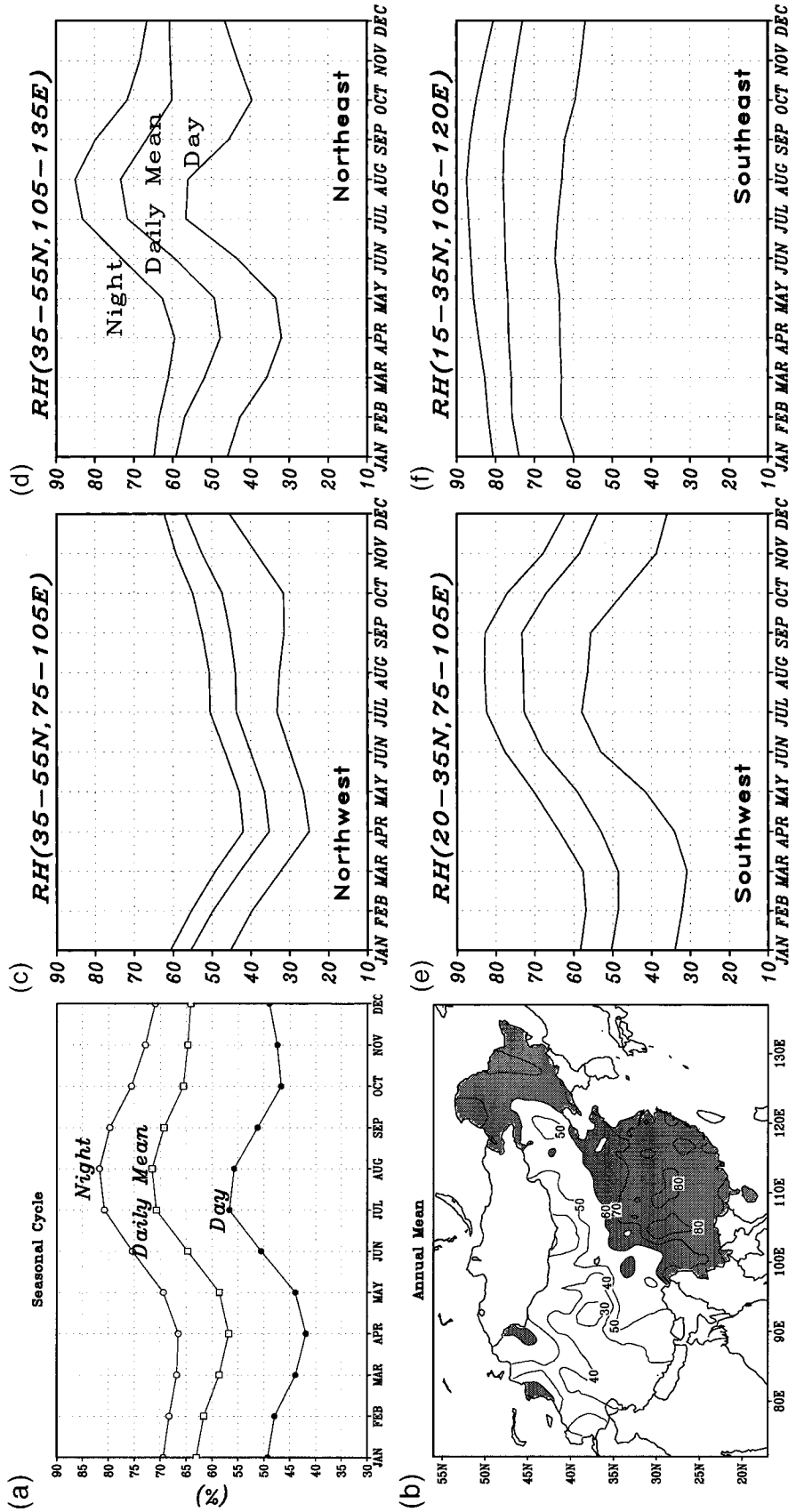

FIG. 5. Climatological relative humidity (%). (a) Seasonal cycle, based on daytime, nighttime, and full-day observations, averaged over all stations. (b) Spatial distribution of annual-mean relative humidity, based on full-day data. (c), (d), (e), (f) Same as (a) but for four regional area averages as indicated.

TABLE 2. Percent variance of climatological monthly means explained by annual and semiannual harmonics. Values are shown for full-day data.

	q (g kg^{-1})	RH (%)	T_d (°C)	T (°C)	T_a (°C)
Annual harmonic	93.9	74.0	98.9	98.9	99.2
Semiannual harmonic	5.2	20.1	0.8	1.1	0.7

largely zonal; it is cold in northern China (including Tibet) and warm in southern China. In summer (JJA), however, high temperatures are found both in the southeast and the northwest, which is largely desert. The patterns in the transitional seasons (Figs. 7b and 7d) resemble the summer pattern more than winter.

In summer, both T and humidity determine human comfort (Steadman 1984). In comparing the JJA maps for T_d (Fig. 6d) and T (Fig. 7c), it is not obvious which regions are subject to the most extreme values of apparent temperature (T_a). As shown in Fig. 7e, summertime daily mean T_a exceeding 30°C occurs over most of southern China south of the Yangtze River, the region with the most stressful summertime heat. The T_a values in this region exceed JJA T values by 2°–3°C (Figs. 7c and 7e). A second region of high T_a is northwestern China (Fig. 7e), where the high values are associated more with high T (Fig. 7c) than with high humidity (Fig. 6d).

4. Trends and decadal variations

Monthly mean values of surface q, RH, T, T_d, and T_a form the basis of 44-yr time series (1951–94) at 196 stations. Based on those data, winter and summer seasonal means, as well as annual means, are computed to evaluate trends and decadal variations. Since the major source of seasonality in China is the contrast between summer and winter monsoon systems, we calculate winter means using data for November–March, and summer means using data for May–September. Separate trend calculations for daytime, nighttime, and full-day mean values are presented. Trends are analyzed using a nonparametric method of median of pairwise slopes regression (Lanzante 1996), which is resistant to outliers in the time series and robust to nonnormal data distributions (Wilks 1995).

a. Spatial distribution of trends in annual means

Shown in Fig. 8 are annual-mean trends in T, q, RH, and T_d, based on full-day data for 1951–94. Temperature trends are predominantly upward (Fig. 8a). The largest and most statistically significant warming trends are in the northeastern region. In southeastern China, the trends are small, of mixed sign, and generally not statistically significant. As mentioned above, one temperature time series was adjusted because of abrupt shifts associated with station moves. The impact of that adjustment was to reduce the magnitude of trends. We also considered the changes in instrument exposure and observation time in the pre-1961 period outlined by Portman (1993). Temperature trends were computed using 1961–94 data for each station. In all cases, the trends differed by no more than 5% (0.01 K decade^{-1}) from the 1951–94 trends. We attribute this high level of agreement to the following three factors: 1) the 1961–94 time period represents 77% of the longer data period; 2) the median of pairwise slopes trend estimation method is not overly influenced by outliers near the beginning of the time series; and 3) changes in observing methods had a relatively small impact on the temperature data. This last point is reinforced by our visual examination of the time series, which showed no obvious evidence of the effects of the changes.

Specific humidity trends for the same period (Fig. 8b) show large increases (exceeding 0.2 g kg^{-1} decade^{-1}) in the northwest and in the Yangtze and Yellow River basins, but the rest of the country shows little evidence of spatially coherent change. Trends in T_d (Fig. 8c) in these regions are also positive. More stations show evidence of statistically significant T_d increases than q increases, particularly at stations with large T trends. Associated with the warming, we find a decrease in RH (Fig. 8d) at more than two-thirds of the stations, due to the more rapid increase in saturation mixing ratio than in actual mixing ratio. The effect of shortening the data period to 1961–94 is a slight increase of the trends, by 3% on average.

Figure 9 summarizes the trends in annual means for the nation and the four regions depicted in Fig. 1. The trends are overwhelmingly positive, except for RH, which shows statistically significant decreases only in the northeast. The largest and most significant trends are in the northeast and northwest regions.

b. Seasonal and diurnal structure of trends

Summer and winter trends in regionally averaged q, RH, T_d, T, and apparent temperature T_a are shown in Fig. 10. In general, trends in winter are larger than trends in summer, especially for the surface temperature T. During summer, T shows no statistically significant regional trends; however, in winter the northeast, northwest, and national average show statistically significant T increases of 0.35°, 0.31°, and 0.23°C decade^{-1}, respectively. Although the summertime T changes are small, in the northwest and northeast they are accompanied by moisture increases that lead to statistically significant increase in T_a.

Figure 11 shows regional trends computed using daytime and nighttime observations separately. Consistent with the findings of Easterling et al. (1997), we find substantially greater nighttime warming, which is reflected in both T and T_a, which increased at a rate of 0.26 K decade^{-1} on national average. Positive q and T_d trends in both daytime and nighttime are associated with RH decreases at night, when most of the warming oc-

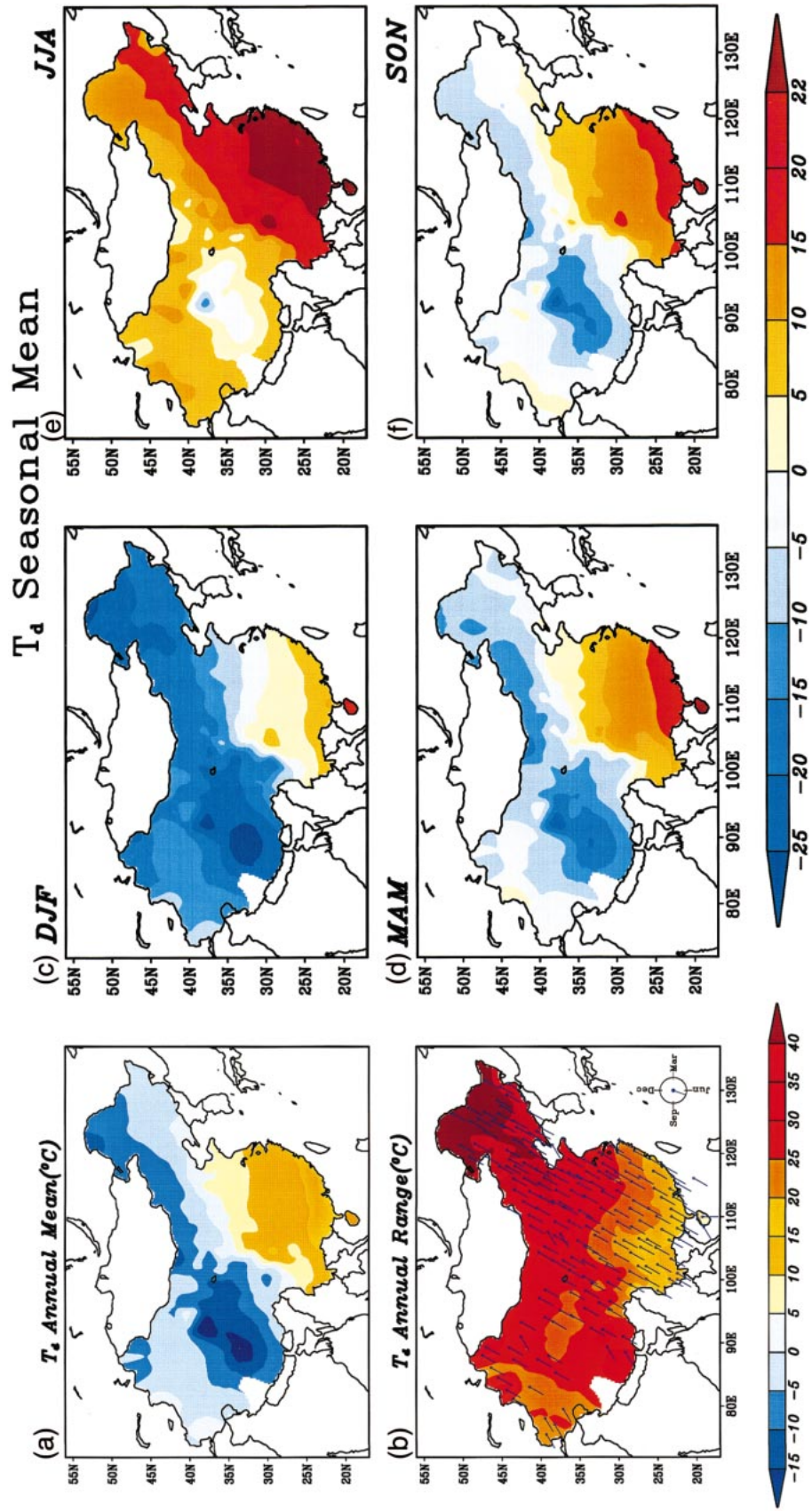

FIG. 6. Same as in Fig. 4, but for dewpoint (°C).

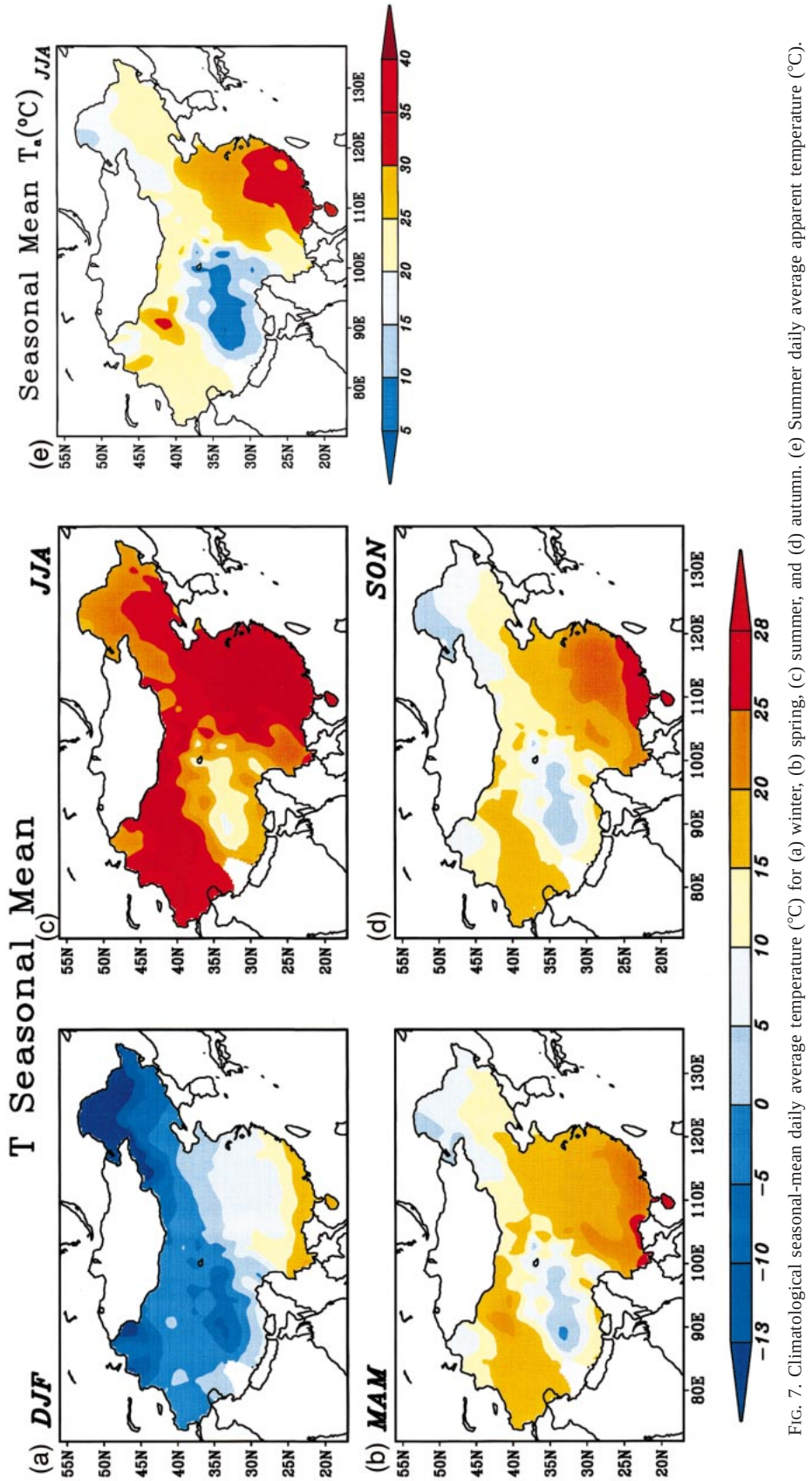

FIG. 7. Climatological seasonal-mean daily average temperature (°C) for (a) winter, (b) spring, (c) summer, and (d) autumn. (e) Summer daily average apparent temperature (°C).

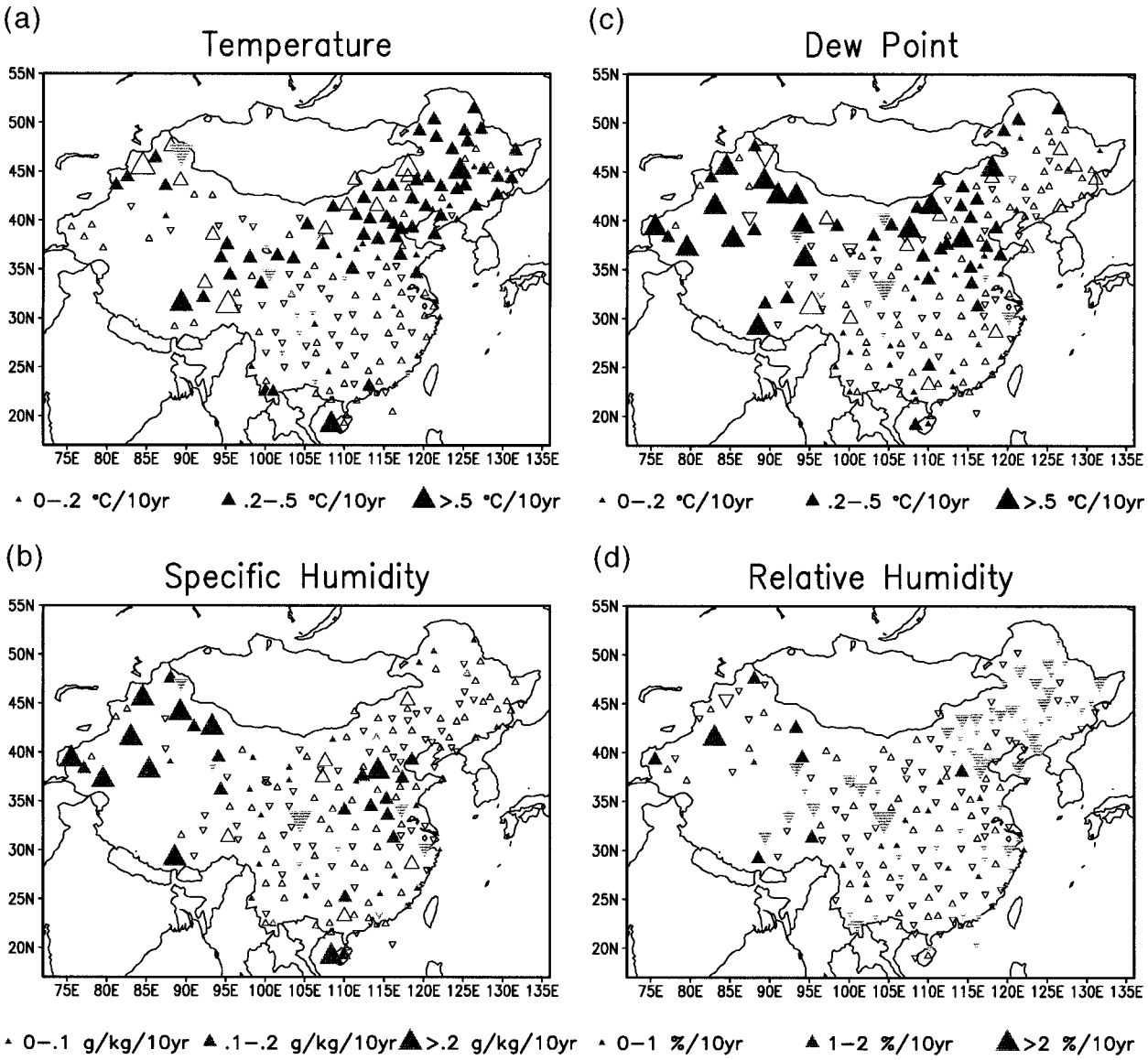

FIG. 8. Decadal trends for 1951–94 in (a) temperature, (b) specific humidity, (c) dewpoint, and (d) relative humidity based on the full-day values. Upward-pointing triangles indicate positive trends and downward-pointing triangles denote negative trends. Magnitudes of trends are proportional to size of triangles, and units are as indicated. Filled triangles indicate statistical significance at the 0.05 confidence level.

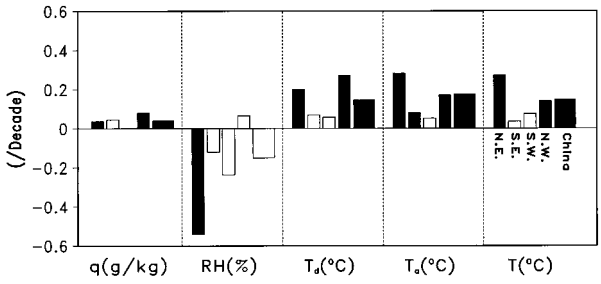

FIG. 9. Decadal regional and national (wider bar) trends in specific humidity, relative humidity, dewpoint, and temperature (°C) for 1951–94, based on full-day data for all months. Trends significant at the 0.05 confidence level are shown in black.

curred, and RH increases during the day, when temperature changes were more modest and cooled in some regions.

c. Decadal variations

Trend estimation is often sensitive to length of data record used. Low-frequency components, such as decadal variations, can contribute to, or mask, underlying trends. Hence, examining trends and decadal variations in the same context is helpful to clarify temporal structure of evaluated trends.

Shown in Fig. 12 are regionally averaged q and T annual anomaly time series, along with their decadal

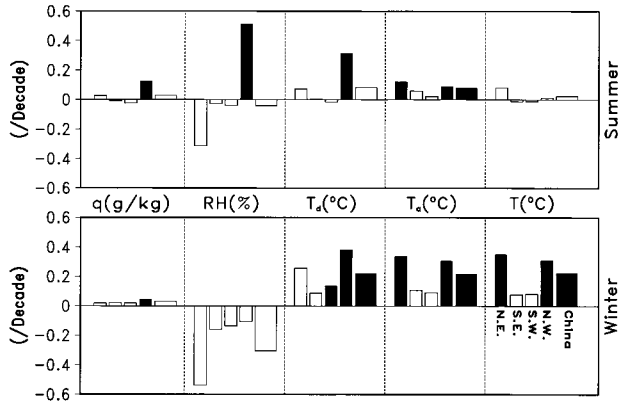

FIG. 10. Same as Fig. 9, but for summer and winter seasons. Trends in apparent temperature are also included.

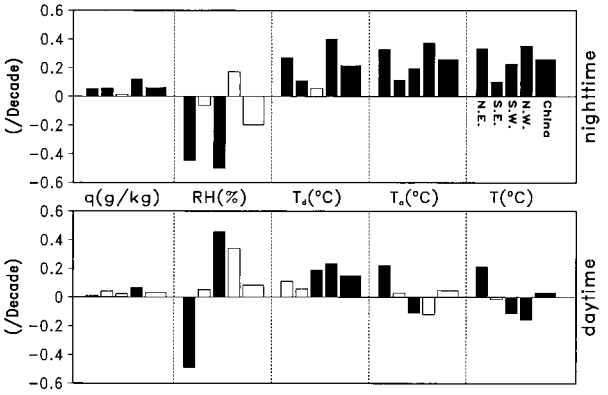

FIG. 11. Same as Fig. 9, but for daytime and nighttime.

components and trends. The decadal component were determined by fitting the data to a sinusoidal function. It is obvious that there are strong decadal variations in both humidity and temperature. The curves illustrate three categories of interaction between the decadal and trend signals. The first is exemplified by the *T* time series for NE China (Fig. 12b), where both the decadal signal and trend are large and where the phase of the decadal variation may impact on evaluation of the trend depending on data period. In this case, the trend explains about 35% of the total variance and the decadal variation accounts 21% (Table 3). The second case is that of a large trend but small decadal variation, as illustrated by the NW China *q* time series (Fig. 12a), where the trend and decadal variation explain 49% and 10% of the interannual variance, respectively (Table 3). The last case is a strong decadal variation and weak trend, as shown in the *q* time series in SW China, where the decadal variation explains 34% of the variance whereas the trend

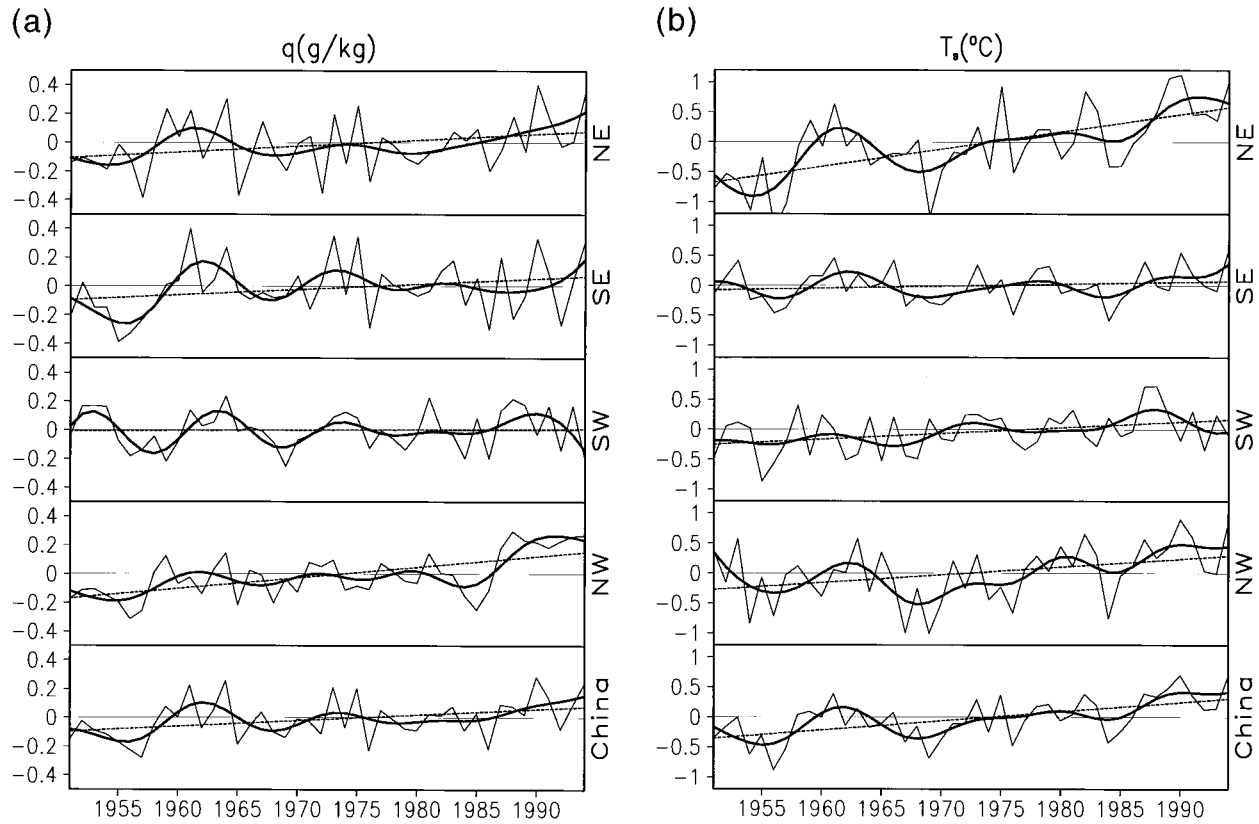

FIG. 12. Regional and national annual anomaly time series of (a) specific humidity and (b) temperature. Heavy solid curves show decadal component, and dashed lines indicate trends.

TABLE 3. Percent variance of specific humidity and temperature interannual variations explained by trend and decadal variations. Values are shown for four regions and for the national average.

		NE	SE	SW	NW	China
Specific Humidity	Trend	13	10	3	49	18
	Decadal variation	9	23	34	10	17
Temperature	Trend	35	8	9	16	29
	Decadal variation	21	18	15	21	23

accounts for only 3%. On nationwide average, trends and decadal variations explain about same amount of variance in both humidity and temperature in China, but there are significant regional differences (Table 3).

5. Conclusions

Using surface observations from 196 stations in China, we have presented 30-yr (1961–90) climatologies of several humidity and temperature variables. Computations were done using daytime observations, nighttime observations, and four observations representing the full-day values. Day–night differences are small (<2%, on average) for specific humidity.

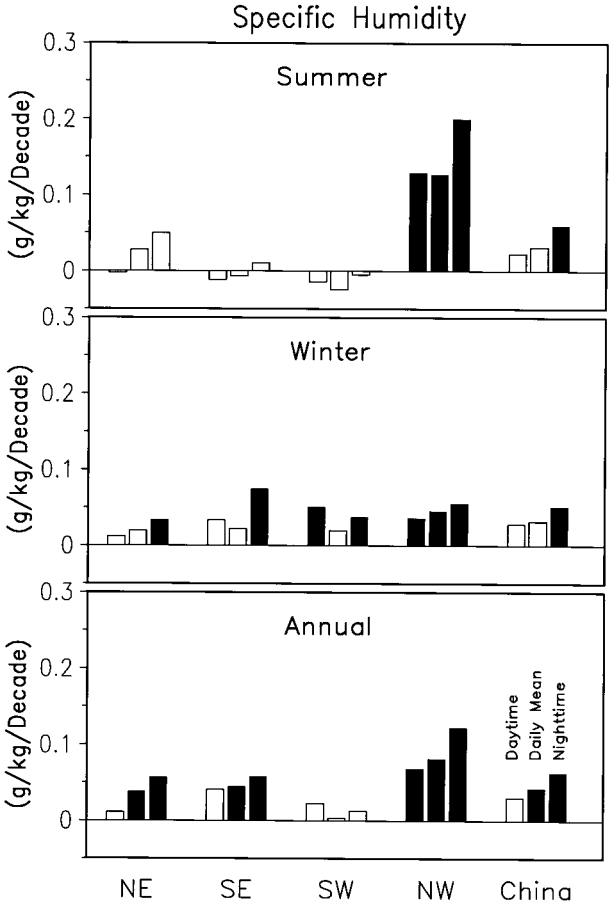

FIG. 13. Regional specific humidity trends for 1951–94 for daytime (left bar), full-day (middle bar), and nighttime (right bar) data. Trends significant at the 0.05 level are shown in black.

The highest climatological humidity and temperature are in southeastern China (south of 35°N and east of 105°E), where the monsoon system dominates, and there are large spatial gradients both northward and westward. The annual harmonic explains most of the seasonal variability in temperature, dewpoint, and specific humidity. However, because of the combined impacts from moisture and temperature, the semiannual harmonic explains a considerable amount of the seasonal variance in relative humidity, especially in northern China and the monsoonal southeastern region (Fig. 5b).

Atmospheric moisture content generally increased in China during 1951–94. More than two-thirds of the stations showed positive trends in specific humidity. The most marked increases were the Xinjing Uygur autonomic region (the northwesternmost province of China), the southern coastal region, and the lower delta of the Yellow River. Of the increasing trends in specific humidity, nighttime values are larger than daytime values, as shown in Fig. 13, which summarizes the regional and seasonal structure of the trends. Humidity trends in the northwest are much larger in summer than in winter, as compared with other regions. For China as a whole, nighttime specific humidity increases were about 1% decade^{-1}, which is statistically significant at the 0.05 confidence level, while the daytime value is only about one-half that magnitude. The results reported here are consistent with those of Kaiser (2000) who examines trends in cloud amount, surface air pressure, surface vapor pressure, and surface relative humidity over China.

Surface temperature has been increasing more dramatically than moisture, with stronger trends in nighttime than in daytime and stronger trends in winter than in summer. These features are summarized in Fig. 14. Upward trends observed in both temperature and humidity, with stronger trends at night than during the day, are consistent with previous studies of maximum and minimum temperature (Karl et al. 1993; Easterling et al. 1997). Increases in summertime humidity are mainly responsible for positive trends of nighttime apparent temperature during the summer.

Acknowledgments. Dale Kaiser from the Oak Ridge National Laboratory (ORNL) generously provided the dataset, which originally came from the China Meteorological Administration, used in this study. Bruce Hicks from the Air Resources Laboratory of NOAA made useful comments and suggestions on the paper.

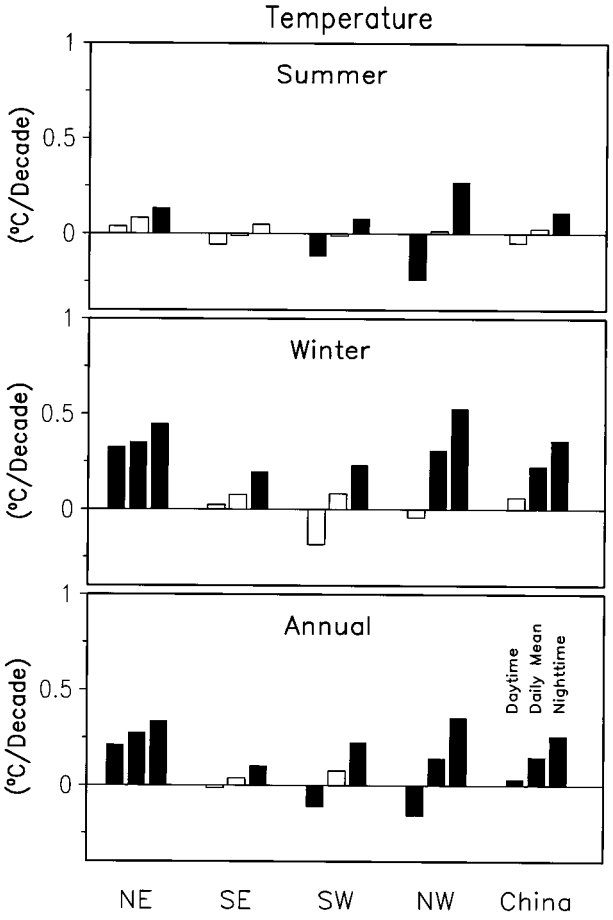

FIG. 14. Same as in Fig. 13, but for temperature.

Comments and suggestions from two anonymous reviewers are greatly appreciated.

REFERENCES

Asakura, T., 1971: Transport and source of water vapor in the northern hemisphere and monsoon Asia. *Water Balance of Monsoon Asia,* M. M. Yushino, Ed., University of Tokyo Press, 27–51.

Chen, J. Y., 1988: *Analysis and Long-Range Forecast of Drought and Flood in China* (in Chinese). Agricultural Press 341 pp.

Easterling, D. R., and Coauthors, 1997: Maximum and minimum temperature for the globe. *Science,* **277,** 364–367.

Gaffen, D. J., and R. J. Ross, 1999: Climatology and trends in U.S. surface humidity and temperature. *J. Climate,* **12,** 811–828.

Kaiser, D. P., 1991: Two long-term instrumental climatic data bases of the People's Republic of China. Oak Ridge National Laboratory ORNL/CDIAC-47, Oak Ridge, TN, 184 pp.

——, 2000: Decreasing cloudiness over China: An updated analysis examining additional variables. *Geophys. Res. Lett.,* **27,** 2193–2196.

Karl, T. R., and Coauthors, 1993: A new perspective on recent global warming: Asymmetric trends of daily maximum and minimum temperature. *Bull. Amer. Meteor. Soc.,* **74,** 1007–1023.

Lanzante, J. R., 1996: Resistant, robust and nonparameteric techniques for analysis of climate data: Theory and examples, including applications to historical radiosonde station data. *Int. J. Climatol.,* **16,** 1197–1226.

Murakami, T., 1957: The general circulation and water-vapor balance over Far East during the rainy season. *Geophys. Mag.,* **29,** 131–171.

New, M., M. Hulme, and P. Jones, 1999: Representing twentieth-century space–time climate variability. Part I: Development of a 1961–90 mean monthly terrestrial climatology. *J. Climate,* **12,** 829–856.

——, ——, and ——, 2000: Representing twentieth-century space–time climate variability. Part II: Development of a 1901–96 monthly grids of terrestrial surface climate. *J. Climate,* **13,** 2217–2238.

Peixoto, J. P., and A. H. Oort, 1996: The climatology of relative humidity in the atmosphere. *J. Climate,* **9,** 3443–3463.

Portman, D. A., 1993: Identifying and correcting urban bias in regional time series: Surface temperature in China's northern plains. *J. Climate,* **6,** 2298–2308.

Randel, D. L., T. H. Vonder Haar, M. A. Ringerud, G. L. Stephens, T. J. Greenwald, and C. L. Combs, 1996: A new global water vapor dataset. *Bull. Amer. Meteor. Soc.,* **77,** 1233–1246.

Ross, R. J., and W. P. Elliott, 1996: Tropospheric water vapor climatology and trends over North America: 1973–93. *J. Climate,* **9,** 3561–3574.

Steadman, R. G., 1984: A universal scale of apparent temperature. *J. Climate Appl. Meteor.,* **23,** 1674–1687.

Tao, S., and L. Chen, 1987: A review of recent research on the east Asian summer monsoon in China. *Monsoon Meteorology,* T. N. Krishnamurti, Ed., Oxford University Press, 60–92.

Wilks, D. S., 1995: *Statistical Methods in the Atmosphere Sciences.* Academic Press, 467 pp.

Zhai, P., and R. E. Eskridge, 1997: Atmospheric water vapor over China. *J. Climate,* **10,** 2643–2652.

——, and F. Ren, 1999: On changes of China's maximum and minimum temperatures in 1951–1990. *Acta Meteor. Sin.,* **13,** 278–290.

——, A. Sun, F. Ren, X. Liu, B. Gao, and Q. Zhang, 1999: Changes of climate extremes in China. *Climatic Change,* **42,** 203–218.

Zhu, B. H., 1962: *Climate of China* (in Chinese). Science Press, 362 pp.